

Thermodynamic diagnostic of quiet sun filament using *IRIS2* inversion code

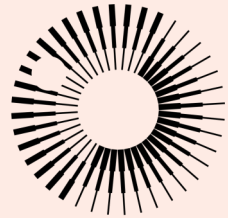
Presentation and interim overview of new data analysis software for filament diagnostics
Submitted to the RAS Early Career Poster Exhibition September 2020

Matthew Docherty¹, Nicolas Labrosse¹

¹School of Physics and Astronomy, University of Glasgow, UK



University
of Glasgow



Introduction

What is a filament and how do we observe them?

Filaments are huge arcs of plasma in the Sun's atmosphere viewed in front of the solar disk. They appear as dark absorption features as they are cooler than the Sun's surface behind them.

Filaments are held in place by powerful magnetic fields in the Sun's atmosphere and usually appear in active regions above sunspots. However, although such observations are rare, viewing them in front of quiet sun conditions allows their complex thermodynamics to be probed directly.

For the past 7 years Nasa's Interface Region Imaging Spectrograph (*IRIS*) has been taking images and spectra of chromospheric phenomena. *IRIS* quiet sun filament observations are so rare that a main focus of this project is to quickly expand its compatibility to more active filament observations.

Model atmospheres from inversion codes

Reconstructing a model atmosphere from observations opens up an exciting new medium for solar chromospheric analysis. To construct such model atmospheres we require an inversion code.

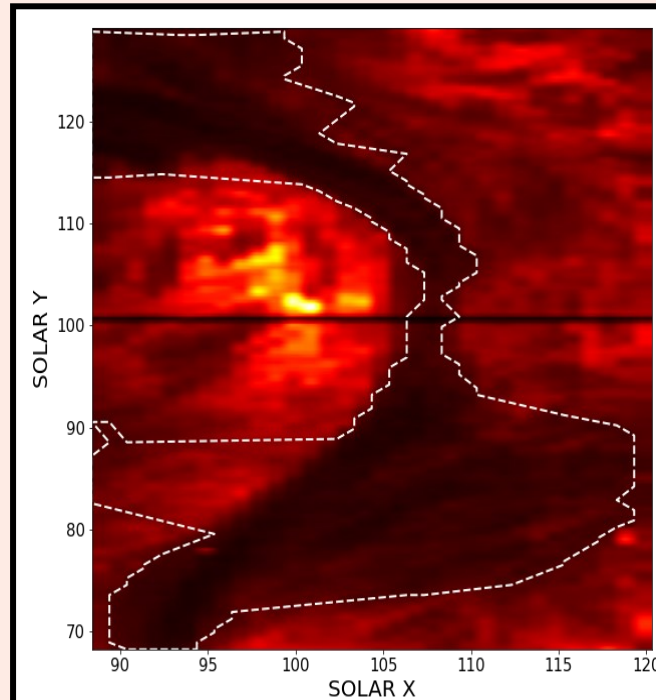


FIG1— Monochromatic image in the core of the Mg II k line at 2795.53 Å. The filament is clearly identified as the dark absorption feature, allowing us to define the mask.

IRIS Observation Fact-File

WHAT—QS Filament OBS 3600106047

WHEN—2018-05-22 08:00:00-08:49:42

WHERE—X,Y: 103",101"

Here we present the *IRIS* Inversion based on *Representative profiles Inverted by STIC* or simply, *IRIS2* (Sainz Dalda, A., et al. (2019)). Where 'STiC' is the Stockholm Inversion Code (de la Cruz Rodriguez, J., et al. (2016)) which assumes non-local thermodynamical equilibrium (Non-LTE) and plane-parallel geometry, on which *IRIS2* is based.

IRIS2 relies on a database of 15,000 solar profiles that correspond to different chromospheric phenomena. And works by taking each pixel of our filament observation and finding its nearest spectral profile in its database then assigning the model atmosphere of the representative profile to our observed pixel to build up a model atmosphere from our observation one pixel at a time.

Project Aims

- Utilise *IRIS2* to probe thermodynamics of a quiet sun filament observation. Specifically, temperature and electron density as a function of optical depth and test for thermodynamic deviations between the quiet sun and filament regions
- Test the suitability of *IRIS2* for filament observations by comparing model atmosphere results to previously obtained empirical data.
- Create and distribute supplementary open-source software to aid with filament diagnostics across a broad range of *IRIS* observations

Method

IDL inversion using *IRIS2*

Using *IRIS2* in SolarSoftware IDL, a single raster of quiet sun observation (See *IRIS Observation Fact-File*) was inverted. Details of inversions are dealt with in *Sainz Dalda, A., et al. (2019)*.

Mask creation

In Python, the high-contrast monochromatic image in FIG1 was used to isolate the filament structure. From here, a primitive threshold was set to separate filament from quiet sun. Then a binary mask was created as an array of 0's for quiet sun and 1's for filament (See FIG2).

Data reduction

Using this binary mask, the model atmospheres created from the inversion were separated pixel-by-pixel into the two solar regions. The averages of each region were also taken to produce an overall thermodynamic progression

Data visualisation

Progressions were plotted pixel-by-pixel (FIG2) and average with uncertainties (FIG3) to present the trend and spread of data. Model atmospheres were then presented (FIG4) with a border mask around it to visually isolate the filament region.

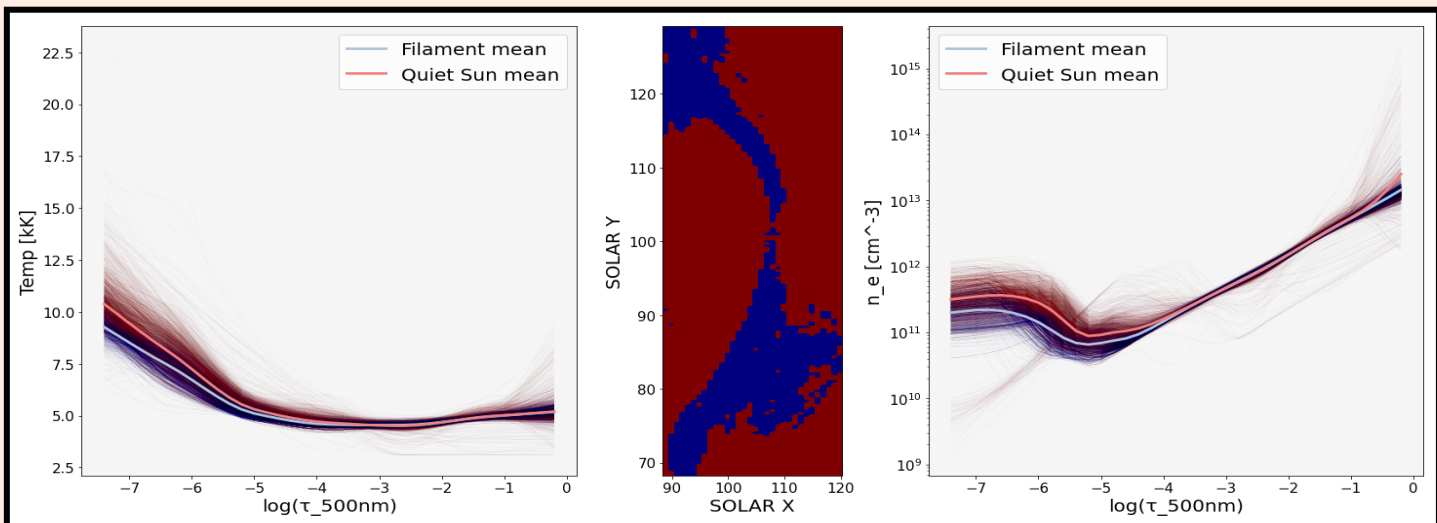


FIG2— Pixel-by-pixel binary thermodynamic progressions. *CENTRE*: binary mask created to differentiate quiet sun and filament pixels, resembling filament structure from monochromatic image. *LEFT*: Temperature map of each pixel from binary mask overlaid, average line graphs for each pixel region shown. *RIGHT*: Electron density map of each pixel, averages overlaid. Progressions show deviation of region averages around optical depth = -4 , with lower temperature and electron density in filament observed.

Results and Discussion

Pixel-by-pixel binary thermodynamic progressions

Centre plot of FIG2 shows binary mask with significant resemblance to filament structure in FIG1. This shows the mask creation methodology is successful. However, comparing the white border in FIG1 to the mask in FIG2 (the border is based upon the mask) we can see that a few residual pixels approx. $x,y = (90,90)$ have altered the border shape significantly. A more sophisticated border extraction from mask is currently being worked on using convolutions of neighbouring pixels and will be implemented for follow-up work (See *Future Work*).

The line graphs in FIG2 illustrate a promising suitability of *IRIS2* for filament observations. Most pixels follow a similar trend in both temperature and electron density. Quiet sun pixels are more sporadic along this trend, which is expected from the complex and dynamic nature of the solar disk. Promisingly, filament pixels are much tighter along the trend illustrating

the more uniform and structured nature of filament arcs. This spread of data along the trend is quantified in FIG3.

Averaged thermodynamic progressions with filament altitude threshold

Both the lines and errors in FIG3 have been averaged across all pixels in the two solar regions. We can see in general, the filament error bars are smaller across temperature and electron density compared to quiet sun. This propagates through from the initial *IRIS2* inversion where fitting each pixel to an *IRIS* database profile returns a χ^2 value. For quiet sun it seems the χ^2 values are higher as the more complex nature of solar disk creates worse-fitting profiles during inversions. We are working to create χ^2 maps for the observations to set a lower limit on 'goodness of fit' and ignoring any pixels that do not meet this limit to see if that has any significant bearing in the spread of data between quiet sun and filament pixels.

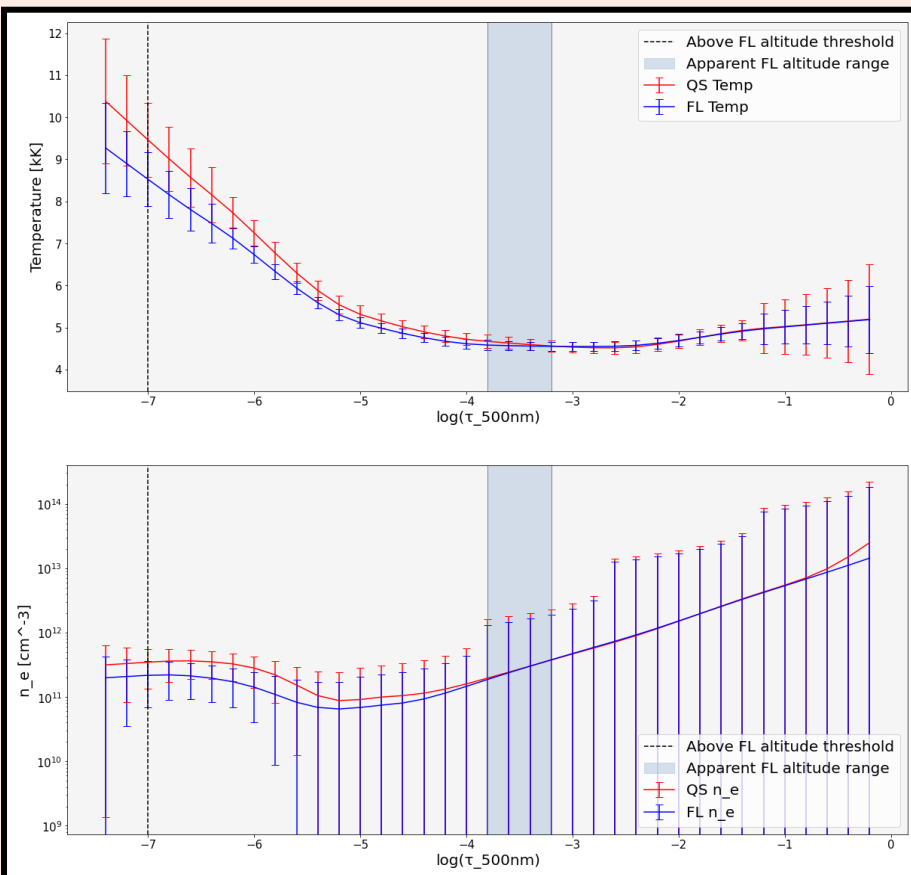


FIG3— Averaged thermodynamic progressions with filament altitude threshold. *TOP*: Temperature map averaged across binary regions with error bars propagated through from initial *IRIS2* inversion. *BOTTOM*: electron density map. Optical depth = -7 with regional line deviation highlighted for model atmospheric analysis.

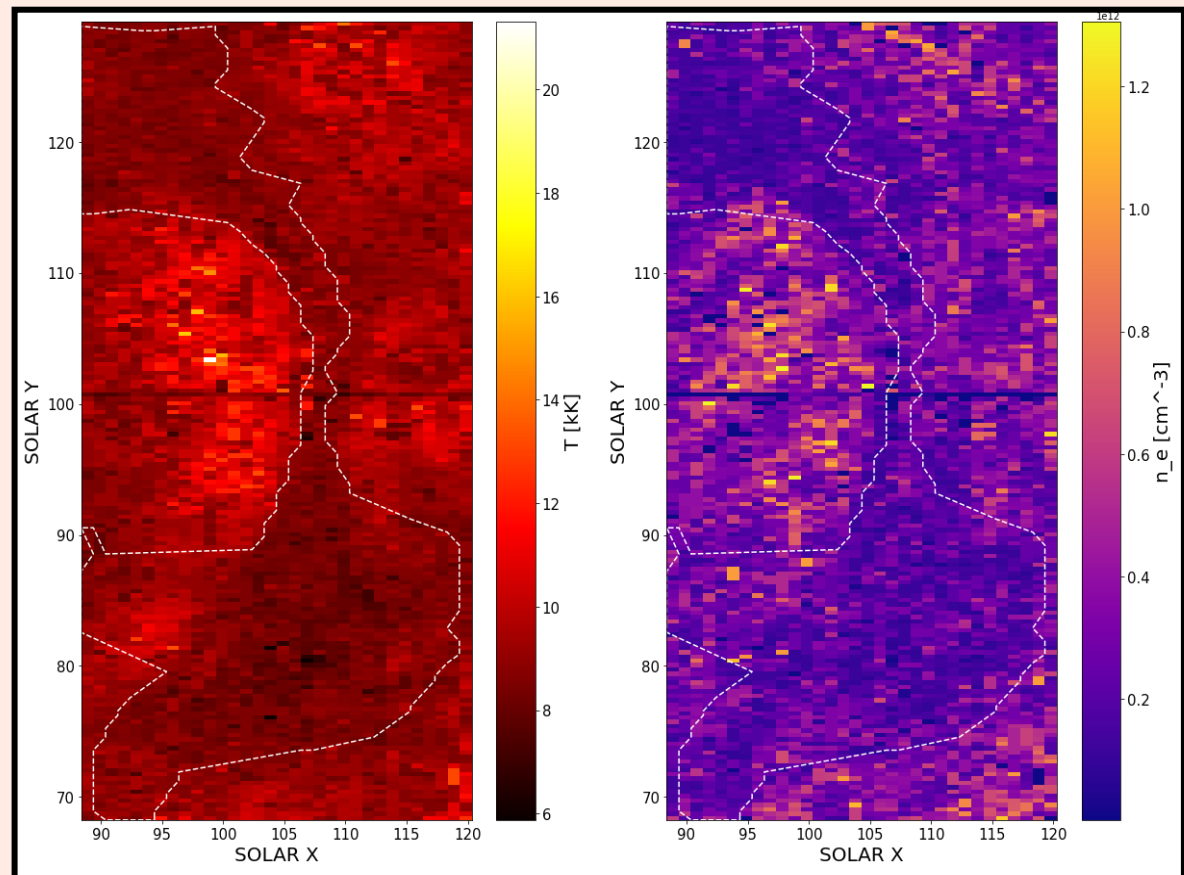


FIG4— Model atmospheric images with mask border at optical depth = -7. *LEFT*: Temperature map. *RIGHT*: Electron density map. Both maps show clear differential between filament and quiet sun with filament pixels enclosed in mask border showing lower temperatures and electron densities. (Animation will be available with full follow-up paper—See **Future Work**)

These chi2 maps are discussed extensively in *Sainz Dalda, A., et al. (2019)*.

An unexpected bi-product of FIG3's thermodynamic progressions is the ability to estimate the threshold altitude of the filament (only as a measurement of optical depth currently—See **Future Work**) where the line plots diverge. Remarkably, this agrees not only between temperature and electron density but also between average line plots and model atmospheres in FIG4

After this threshold, the line plots indicate the filament plasma is cooler with lower electron density than the surrounding solar disk. We can see a temperature deficit of more than 1000 K in the upper-atmosphere between filament and quiet sun. Promisingly, this agrees with empirical data (*Levens, P, J., et al. (2019)*) where filament temperatures rarely exceeded 10 kK. Similar comparative quantitative data is harder to come by for electron density but solely-based on

temperature, *IRIS2* inversion data successfully agrees with expectations.

Model atmospheric images with mask border

FIG4 presents model atmospheres at an optical depth corresponding to these significant thermodynamic deviations between filament and quiet sun. It is clear that within the mask border region, both temperature and electron density are lower than their surroundings. Note, the profile actually matches the binary mask in FIG2 better than the white border so a better border method will be required in future. At optical depths near the filament threshold range, the model atmosphere profiles become less clear which is a strong indicator that we can estimate filament altitude from this data once non-LTE conversions are carried out (See **Future Work**).

Conclusion

We have presented first of their kind temperature and electron density diagnostics for a quiet sun filament.

We have shown that filament temperature data from *IRIS2* inversion agrees with the soft-limit of 10,000 K when compared to empirical data.

We have identified the differential spread of data for each pixel in the two solar regions and have made suggestions that could account for this (complex solar disc, poorly fitting quiet sun profiles) and have suggested future methods to decipher which is the most probable cause.

These thermodynamic progressions have also illustrated the ability to directly estimate the chromospheric altitude of the filament, which will become very useful after an optical depth conversion to altitude.

We have shown primitive success in our automated filament mask extraction process with captures the general shape of filament but requires more attention to allow for a nice mask border to be extrapolated from it.

We have also shown, with confidence, the ability of *IRIS2* to work with and invert filament data. This inaugural verification will hopefully open doors for chromospheric analysis in the future

References

- de la Cruz Rodriguez, J., Leenaarts, J., & Asensio Ramos, A. *ApJ*, 830, L30 (2016)
Levens, P, J., Labrosse, N. *A&A* 625, A30 (2019)
Sainz Dalda, A., de la Cruz Rodriguez, J., De Pontieu, B., & Gosic, M. *ApJ*, 875, L18 (2019)
Wittmann, A. *Sol. Phys.*, 35, 11–29, (1974)

Future Work

Optical depth to chromospheric altitude conversion

Optical depth conversion to chromospheric altitude would provide a more practical diagnostic on thermodynamic progressions. A primitive attempt was made using the Wittman equation of state (*Wittman, A. (1974)*) however, the LTE assumptions stifled any useful differentials between solar regions. We are in the process of finding a Non-LTE conversion process which is significantly more CPU-heavy than the LTE.

Robustness and versatility tests

The key to making this software versatile across different types of filament observations (plages, active regions, etc.) is the automation of the filament mask extraction process. We are currently in the process of using histogram profiles of monochromatic images to find a highly adaptive method of filament extraction. Once confident, numerous tests will be carried out on a broad range of filament observation types.

Open-source software release

Once these two main demands have been reached a full paper will be released with supplementary open-source software at github.com/mdochertyastro/iris2_fl written in Python and IDL. As a new *IRIS2* version release is expected late-September 2020. We are aiming to release our follow-up paper and software in late-2020.

Get in touch

Any questions, comments or suggestions? I'd love to hear from you:

Twitter: @mdocherty_astro

Institute email: 2259886d@student.gla.ac.uk

Personal email: matthewdocherty@live.co.uk

ResearchGate: Matthew_Docherty2